CONVECTION AND RADIATION HEAT TRANSFER ANALYSIS IN THREE-DIMENSIONAL ARRAYS OF ELECTRONIC COMPONENTS

Ramiro H. Bravo
Department of Mechanical and Aerospace Engineering
Tri-State University, Angola, Indiana 46703-0307

Alejo Sanchez
Department of Mechanical Engineering
Universidad de Los Andes, Merida, Venezuela.

Ching-Jen Chen and Theodore F. Smith
Department of Mechanical Engineering
The University of Iowa, Iowa City, Iowa 52242.

1. ABSTRACT

In this study, the combined effect of convection and radiation heat transfers is studied in an array of electronic chips mounted between two parallel plates. The chips are cooled by a radiatively non-participating gas flowing inside the passage. The three-dimensional convection part of the problem was solved using the 19-point Finite Analytic Method and the radiation analysis using the Discrete Ordinates Method. Results showing the effects of convection alone and combined radiation and convection are presented. For the geometry and conditions studied here, radiation heat transfer represents 33% of the total heat transfer.

2. INTRODUCTION

Since the development of the first electronic digital computer, heat transfer analysis played an important role in the design of its components. The use of the large-scale integration technologies to the very large-integration increased the heat dissipated by these systems. Such increase has made the role of heat transfer more and more important. Further development of high speed circuits could be limited by the inability to maintain effective cooling.

One of the most common electronic equipment configurations involves forced convection in parallel plate channels. In this configuration, an array of heat dissipating components are mounted to plates as shown in figure 1. Heat transfer from the array is influenced by forced convection to the coolant, conduction to the plate and by radiation exchange among surfaces.

The reduction in size and the increase in power of these components created the necessity to refine the methods in heat transfer analysis. Initially, Sparrow, Niethmmer and Chaboki (1982) measured the pressure drop and heat transfer in an array of heat generating blocks similar to the ones displayed in Figure 1. They used the naphthalene sublimation technique to determine the average heat transfer coefficient. In addition, they studied the effect of missing modules and the presence of barriers inside the channel. Their results were obtained for Reynolds numbers of 2000, 3700 and 7000. Later, Braaten and Patankar (1985) studied a similar problem of an array of rectangular blocks by a numerical method. To simplify the three-dimensional character of the problem, they assumed a negligible separation between modules in the streamwise direction. As a consequence, they were able to assume fully developed flow in this direction and reduce the problem to two dimensions. They solved the two-dimensional governing equations by the control volume numerical method. Asako and Faghri (1988) studied also a similar problem of laminar forced convection heat transfer using the control volume method. However, they considered in their analysis the full three dimensional governing equations. To simplify the domain of solution, they assumed periodic fully developed flow, a concept that was introduced before by Patankar, Liu and Sparrow(1977). Lately, Shaw, Chen and Chen (1991) studied the mixed-convective heat transfer phenomena in the entrance of a three-dimensional channel with one heated element.

This study analyses the combined effect of convection and radiation heat transfer in the array of electronic chips displayed in figure 1. The fluid is considered radiatively non-participant with constant properties. As a result, the divergence of the radiative heat flux vector vanishes, and the transport and radiation models become explicitly decoupled. Implicitly however, the two models are interdependent through the temperature field and the wall heat fluxes. Due to the relatively low coolant flow rates and small physical dimensions of the components and the passages, the flow is also assumed laminar. To the author's knowledge this is the first three-dimensional analysis which includes convection-radiation heat transfers.

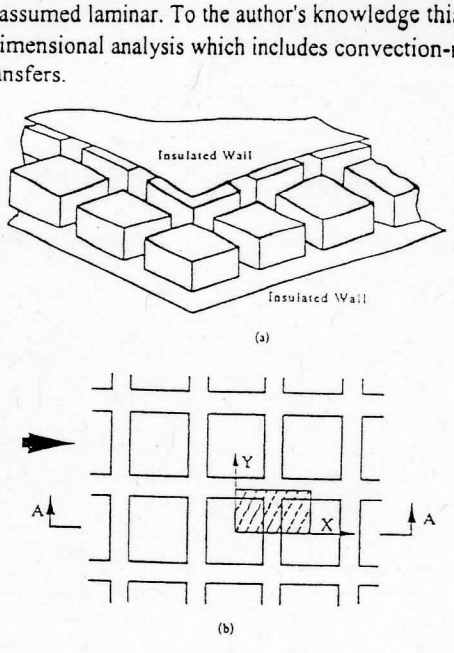

Figure 1. Heat Transfer of Electronic Components

3. DEFINITION OF THE PROBLEM

The problem to be considered in this study is depicted schematically in figure 1. It involves the determination of three-dimensional heat transfer and fluid flow characteristics for laminar forced convection-radiation cooling of an array of square heat-generating modules. The modules are positioned along one wall of a thermally insulated parallel wall channel. Each square module

CH3096-5/92/0000- 0149 $1.00 ©1992 IEEE

has a length of 2.4 cm and height 0.9 cm. The separation gap between them is equal to 0.6cm and the gap between the module and the opposite wall is 1.5 cm.

The domain of numerical solution can be greatly simplified using the concepts of symmetric and periodic fully developed flow. After a defined number of modules Patankar, Liu and Sparrow(1977) reported that the flow becomes periodic, i.e., the velocity, a reduced pressure and a reduced temperature field become periodic. This notion is an extension of the fully developed concept used in flows inside ducts of uniform cross section (Chapman, 1987). Besides periodicity, it is reasonable to assume symmetry with respect to some planes in the spanwise direction. With this assumptions it is possible to simplify the geometry of this problem and reduce the computational domain to the one represented in figures 1(b), 1(c) and 2. The fluid flow is in the positive x direction with a Reynolds Number of 100. The planes at y=0.0 and at y=1.5 are considered planes of symmetry, and the top and bottom walls are regarded adiabatic. To solve the radiation problem, the fluid is considered air with an inlet temperature of 305 K. All surfaces are assumed black with the temperature of the blocks constant and equal to 320 K.

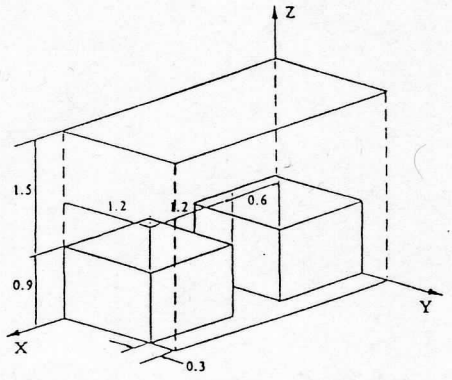

Figure 2. Domain of Solution of the Electronic Component Shown in Figure 1.

4. GOVERNING EQUATIONS

In a duct limited by a boundary of periodic cross section, the flow inside presents two characteristic patterns. An entrance region where the flow is in a developing process and a fully developed region where the velocity components exhibit a periodic behavior (Sparrow, Niethmmer and Chaboki,1982). In the last case, this periodicity in the flow field can be represented by

$$\begin{aligned} U(x,y,z) &= U(x+L,y,z) = U(x+2L,y,z) = \ldots \\ V(x,y,z) &= V(x+L,y,z) = V(x+2L,y,z) = \ldots \\ W(x,y,z) &= W(x+L,y,z) = W(x+2L,y,z) = \ldots \end{aligned} \quad (1)$$

where L is the period of the boundary along the x direction. The pressure does not obey the same periodicity of the velocity field. However, if constant properties of the fluid are assumed, the drop in pressure between consecutive domains of length L is always the same and

$$p(x,y,z) - p(x+L,y,z) = p(x+L,y,z) - p(x+2L,y,z) = \ldots$$

or $p(x,y,z) - p(x+L,y,z) = -\alpha L$ with α constant. As a result, the pressure field can be divided in two components

$$p(x,y,z) = -\alpha x + P(x,y,z) \quad (2)$$

The αx term is related to the global mass flow and $P(x,y,z)$ is related to the detailed local motion. Using these properties, and neglecting buoyancy, the governing equations for laminar flow can be written as

$$\frac{\partial U}{\partial x} + \frac{\partial V}{\partial y} + \frac{\partial W}{\partial z} = 0 \quad (3a)$$

$$\frac{\partial U}{\partial t} + U\frac{\partial U}{\partial x} + V\frac{\partial U}{\partial y} + W\frac{\partial U}{\partial z} = \alpha - \frac{1}{\rho_0}\frac{\partial P}{\partial x} + \nu\left[\frac{\partial^2 U}{\partial x^2} + \frac{\partial^2 U}{\partial y^2} + \frac{\partial^2 U}{\partial z^2}\right] \quad (3b)$$

$$\frac{\partial V}{\partial t} + U\frac{\partial V}{\partial x} + V\frac{\partial V}{\partial y} + W\frac{\partial V}{\partial z} = -\frac{1}{\rho_0}\frac{\partial P}{\partial y} + \nu\left[\frac{\partial^2 V}{\partial x^2} + \frac{\partial^2 V}{\partial y^2} + \frac{\partial^2 V}{\partial z^2}\right] \quad (3c)$$

$$\frac{\partial W}{\partial t} + U\frac{\partial W}{\partial x} + V\frac{\partial W}{\partial y} + W\frac{\partial W}{\partial z} = -\frac{1}{\rho_0}\frac{\partial P}{\partial z} + \nu\left[\frac{\partial^2 W}{\partial x^2} + \frac{\partial^2 W}{\partial y^2} + \frac{\partial^2 W}{\partial z^2}\right] \quad (3d)$$

Equations (3a) through (3d) are decoupled from the energy equation and the fluid field can be solved independently. The boundary conditions for these equations are

$U = V = W = 0.0$ on solid boundaries and

V_n and $\dfrac{\partial U}{\partial n} = 0.0$ on symmetrical bounding surfaces.

$U_{inlet} = U_{outlet}$, $V_{inlet} = V_{outlet}$, $W_{inlet} = W_{outlet}$

The extension of this concept to a thermally developed regime for a flow of periodically varying cross section is based on the same idea (Patankar, Liu and Sparrow 1977). A new dimensionless temperature is defined by

$$\theta(x,y,z) = \frac{T(x,y,z) - T_w}{T_{bx} - T_w}. \quad (4)$$

where the local reference temperature T_{bx}, defined to take account of possible recirculation zones where U is negative, is

$$T_{bx} = \frac{\int_A T|U|dA}{\int_A |U|dA}. \quad (5)$$

Here A is the area of the cross section at x.
In fully developed periodic flow, the shapes of the temperature profiles at successive streamwise locations separated by the periodic length L are the same. In terms of the temperature variable θ, this similarity condition is expressed as

$$\theta(x,y,z) = \theta(x+L,y,z) = \theta(x+2L,y,z) = \ldots \quad (6)$$

If an element of length L is selected as domain of solution, this equation provides a relation between the inlet and outlet conditions for the element, ie.,

$$\theta_i = \theta(inlet,y,z) = \theta(outlet,y,z) = \theta_o$$

However, to solve the energy equation numerically, it is more convenient to define a new variable directly related to θ. This variable is defined by

$$\phi(x,y,z) = \frac{T(x,y,z) - T_w}{T_{bi} - T_w} \quad (7)$$

where T_{bi} is the inlet bulk temperature defined in equation (4) and T_w is the temperature on the surface of the blocks. Replacing ϕ

instead of T in the energy equation, the resulting governing equation become

$$\frac{\partial \phi}{\partial t} + U\frac{\partial \phi}{\partial x} + V\frac{\partial \phi}{\partial y} + W\frac{\partial \phi}{\partial z} = \alpha\left[\frac{\partial^2 \phi}{\partial x^2} + \frac{\partial^2 \phi}{\partial y^2} + \frac{\partial^2 \phi}{\partial z^2}\right] \quad (8)$$

with $\alpha = \frac{K}{\rho C_p}$ the coefficient of thermal diffusion. The inlet and outlet conditions can be obtained from the previous definition of dimensionless temperature θ, equation (4), and the definition of a dimensionless bulk temperature

$$\phi_{bx} = \frac{A\int \phi |U| dA}{A\int |U| dA}. \quad (9)$$

These conditions are

$$\phi_i = \phi_o\left(\frac{\phi_{bi}}{\phi_{bo}}\right) \quad \text{and} \quad \phi_{bi} = 1.0. \quad (10)$$

The remaining boundary conditions on the bounding surfaces are:

$\phi_w = 0.0$ on the lateral walls and

$\frac{\partial \phi}{\partial z} = 0.0$ on the planes of symmetry

In the radiation analysis, the medium is radiatively non-participating and, therefore, all the radiation effects are due to the gray, diffusely emitting and reflecting surrounding surfaces. The governing equation of monochromatic radiative transfer is (Siegel and Howell, 1981, Smith, 1990)

$$\frac{dI_\lambda}{d\zeta} = -(a_\lambda + s_\lambda)I_\lambda(\zeta) + a_\lambda I_{b\lambda}(\zeta, T) + \frac{s_\lambda}{4\pi}\int_0^{4\pi} I_\lambda(\zeta, \omega_i)\,\Phi(\lambda, \omega, \omega_i)\,d\omega_i \quad (11)$$

where

$\frac{dI_\lambda}{d\zeta}$ is the variation of monochromatic intensity along the line of sight direction ζ.

a_λ is the monochromatic absorption coefficient.

s_λ the monochromatic scattering coefficient.

$(a_\lambda + s_\lambda)I_\lambda(\zeta)$ the attenuation of monochromatic intensity along z due to the absorption and outward scattering characteristics of the medium.

$a_\lambda I_{b\lambda}(\zeta, T)$ is the augmentation of monochromatic intensity into z due to emission in the medium.

$\frac{s_\lambda}{4\pi}\int_0^{4\pi} I_\lambda(\zeta, \omega_i)\,\Phi(\lambda, \omega, \omega_i)\,d\omega_i$ is the augmentation of monochromatic intensity due to inward scattering of the incoming radiant energy into z.

$I_{b\lambda}$ is the monochromatic blackbody radiant intensity, ω_i is the incident solid angle, and Φ is the scattering phase function. The solution was obtained for the limiting cases $a_\lambda = 0.0$ and $s_\lambda = 0.0$.

5. NUMERICAL SOLUTION

The solution was obtained using a new program FANS-3D (Bravo,1991) based on the 19-point three dimensional Finite Analytic Method (Chen, Bravo and Xu,1991). In this program the momentum and energy equations are discretized using the 19-point Finite Analytic Method (FAM). The coupling between the continuity and momentum equations is handled using the SIMPLER (Patankar,1980) approach. Under the assumption of fluid with constant properties mentioned earlier, the velocity and pressure fields were obtained before solving the temperature field. The coupling between radiation and convection was treated by energy balances on the walls. Since the walls are insulated by hypothesis, the net energy absorbed by the wall was considered equal to the energy leaving by convection.

The discrete ordinates method (Fiveland, 1987) was used to solve equation (11) for the intensity. In this method, equation (11) is discretized as

$$I_i^p = \frac{\mu_i A_{n,s} I_i^w + \delta_i A_{e,w} I_i^s + \gamma_i A_{f,b} I_i^b + \alpha(S_1 + S_2)\Delta V_p}{\mu_i A_{n,s} + \delta_i A_{e,w} + \gamma_i A_{f,b} + \alpha\beta\Delta V_p} \quad (12)$$

subject to

$$I_i^p = \alpha I_i^{xe} + (1-\alpha)I_i^w = \alpha I_i^{ye} + (1-\alpha)I_i^{yr} + = \alpha I_i^{ze} + (1-\alpha)I_i^{zr} \quad (13)$$

where

$$S_1 = (1-\Omega)\beta I_b^p = aI_b^p$$
$$S_2 = \frac{s}{4\pi}\sum_j w_j I_j^p \Phi_{ij} \quad (14)$$

In equations (12) to (14), α is a spatial interpolating weight, and w_j are the weights for the integration procedure. $A_{n,s}, A_{e,w}$ and ΔV_p are, respectively, the north-south and east-west areas of the element control volume where equation (12) is being applied. I_i^p is the outgoing intensity in the discrete direction i at the center (p) of that grid element, and the superscripts xr and xe indicate the reference (where energy originates) and end (where energy arrives) faces for the coordinate direction x. Similarly for the y- and z-directions.

The boundary conditions for equation (12) at any solid surface k and for any discrete direction i is

$$I_i = \varepsilon I_b + \frac{(1-\varepsilon)}{\pi}\sum_j w_j \psi_j I_j \quad (15)$$

where ε is the surface emittance, and ψ is the cosine of the angle between the normal to the surface and the direction of the incident intensity. In equation (15), subindex i indicates a direction going from the surface toward the internal medium while subindex j indicates directions going from the medium toward the surface.

One of the advantages of the discrete-ordinates method is the fact that it provides, after each iteration and without any extra effort, the solution for the whole intensity field. This characteristic of the method allows for the simulation of symmetric and periodic boundaries. The required boundary conditions are:

$$I_i = I_{i'} \quad \text{for symmetric boundaries} \quad (16)$$
$$I_i^a = I_i^{a'} \quad \text{for periodic boundaries} \quad (17)$$

where subscripts i and i' indicate mirroring directions and superscripts a and a' indicate boundaries facing each other. The net radiation fluxes at any solid surface are evaluated as

$$q_k = \sum_j w_j \psi_j I_j \quad (18)$$

where the summation is performed over all the discrete directions.

When the medium is non-participating, the divergence of the radiative heat flux vector vanishes, and the transport and radiation models become explicitly decoupled. Implicitly, however, the two models are interdependent through the temperature field and the wall heat fluxes. The radiation part of the problem, equations (12) through (18), were solved using the radiative heat transfer code, ANDISORD4 (Sanchez, Smith & Krajewski, 1990). With this code, an S-8 implementation (80 discrete directions) of the

discrete-ordinates model was applied. Although not required, the same grid was used for the flow and radiation models.

6. RESULTS OF COMPUTATION

The results for the flow field computation are shown in figures 3 through 8. The velocity profiles for the u component are shown in figure 3 at two locations, at the inlet and at the center between modules. The top and front views of these profiles are displayed in figures 3(b) and 3(c). These figures show that the velocity between modules and the upper plate is similar to the velocity profile in a fully developed flow between two plates, or Poiseuille flow. The velocity has a profile nearly parabolic with a maximum at the center region. The magnitude of velocity in this upper region is much bigger than the magnitude of velocity in the lower region. However, this last area contains most of the heat transfer area of the modules and further study is required.

Figure 4 through 8 display velocity vectors on different planes. Figure 4 shows them on the front plane of symmetry. The flow between modules rotates counter-clockwise driven by the external flow. The magnitude of the velocity vectors shows a remarkable difference in velocity between the upper and lower regions again. Figures 5, 6 and 7 show velocity vectors on horizontal planes located at different heights z. In these figures, we can appreciate that the flow between modules has a very complex pattern. While some portions of fluid rotate, some others are entrained from the top of the blocks and transported to the lower sides.

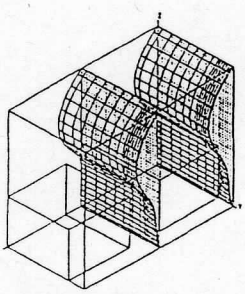

(a) 3-D View

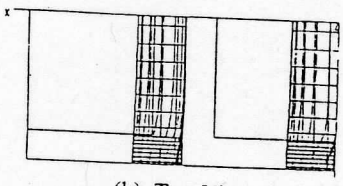

(b) Top View

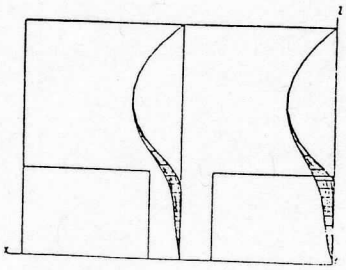

(c) Front View

Figure 3. Profiles of Velocity Component U

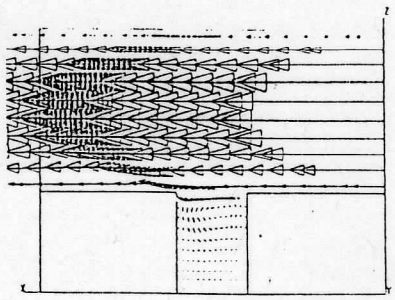

Figure 4. Velocity Vectors on Plane of Symmetry y = 0

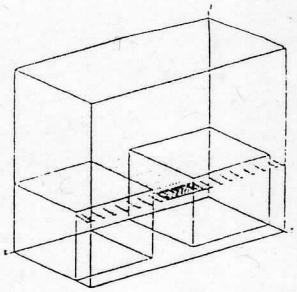

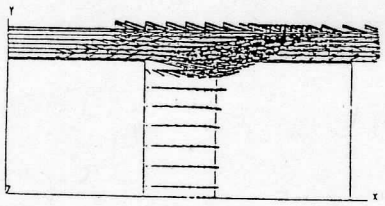

Figure 5. Velocity Vectors on Plane z = 0.855

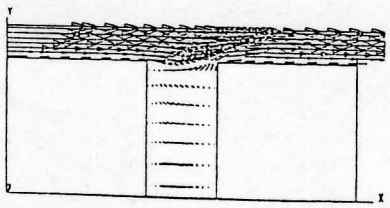

Figure 6. Velocity Vectors on Plane z = 0.675

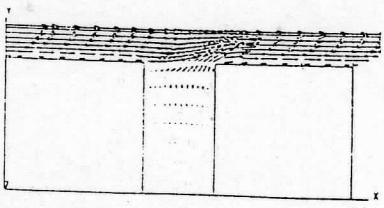

Figure 7. Velocity Vectors on Plane z = 0.315

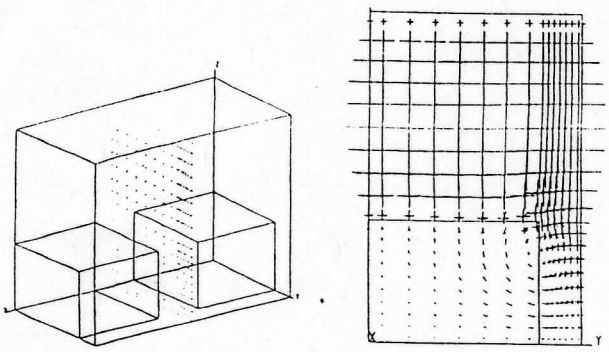

Figure 8. Velocity Vectors on Plane x = 1.5

Profiles of dimensionless temperature ϕ on three different planes are shown in figures 9 and 10. The value of temperature ϕ on the surface of the blocks is zero and the value of the bulk temperature at the inlet is equal to one. Figure 9 shows these profiles when only convection heat transfer is considered. As expected, the profiles of temperature are perpendicular to the top and bottom insulated plates, which can be better appreciated in the lateral view

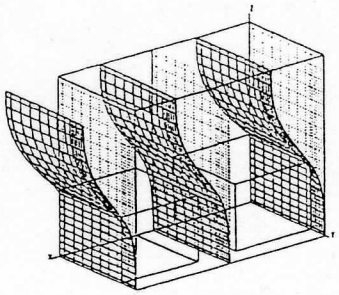

(a) 3-D View

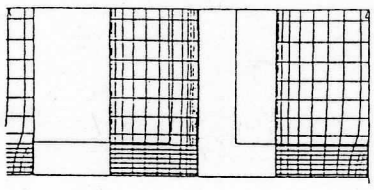

(b) Top View

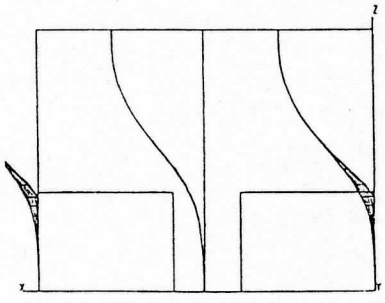

(c) Front View

Figure 9. Dimensionless Temperature Profiles
Conduction-Convection Problem

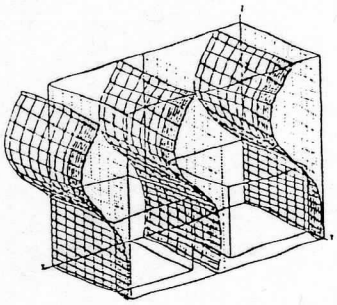

(a) 3-D View

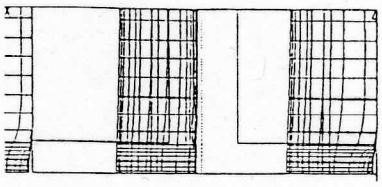

(b) Top View

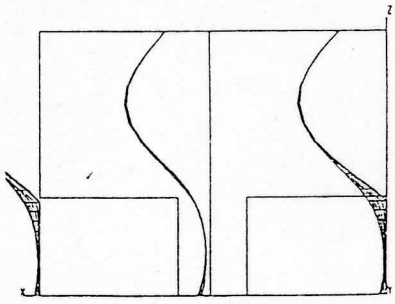

(c) Front View

Figure 10. Dimensionless Temperature Profiles
Conduction-Convection-Radiation Problem

in figure 9(c). This figure also shows that the fluid moving between the blocks has a temperature very close to the temperature of the blocks. Specifically, the fluid near the bottom wall has almost the same temperature of the blocks. The maximum dimensionless temperature ϕ (coldest dimensional temperature) is on the top insulated wall.

Figure 10 shows dimensionless temperature profiles when convection and radiation are included. The temperature profiles in this case are quite different from the ones discussed for convection alone in figure 9. The top insulated plate does not have the maximum value of ϕ, Instead, it has an intermediate temperature between the temperature of the blocks and the temperature in the center region. The maximum value of ϕ is in the center region between the top plate and the top surface of the modules. This effect can be better appreciated in the front view shown in figure 10(c). The higher temperature on the top plate (and the lower temperature on the bottom plate) is due to the radiation effect; the top plate receives a net radiating energy coming from the blocks and the bottom plate. Since this plate is insulated, this incident net radiant energy is dissipated by convection, indicated by a positive slope of the profile at this point. The ϕ profile has a maximum in the center region and decreases as we move closer the bottom plate. However, close to this plate this profile increases again. This in-

crease suggests that heat is transfer by convection from the fluid to the bottom wall. Because this wall is insulated, the same amount of energy is irradiated to the top wall. Figure 10 (b) also shows the top view of these dimensionless temperature profiles.

An energy balance when convection-radiation heat transfer was considered shows an increase on the rate of heat transfer of 49.1% compared with the computation considering only convection heat transfer. It is quite normal to neglect radiation in a normal forced convection radiation analysis, the reason being, that the convection part is much bigger than the radiation. This study shows that this is not always the case, specially when the flow field contains large regions of low velocity. This is the situation if the modules are attached to the lower plate very close to each other. The slow velocity of flow between modules creates a low convection heat transfer in this region and an increasing contribution from radiation. In this situation, radiation heat transfer is very important and should be considered.

7. CONCLUSION

In this study, the combined effect of convection and radiation heat transfers in an array of electronic chips is examined. The chips are cooled by a radiatively non-participating gas flowing around them. The problem is solved combining a new Finite Analytic Formulation with the Discrete Ordinates Method. The three-dimensional numerical solution shows that radiation can contribute with a significant part in the overall heat transfer process. For the geometry and conditions studied here, radiation heat transfer represents 33% of the total heat transfer.

8. REFERENCES

Asako, Y. and Faghri, M., (1988),"Three- dimensional heat transfer and fluid flow analysis of arrays of square blocks encountered in electronic equipment," Numerical Heat Transfer, Vol. 13, pp. 481-498.

Braaten, M. E. and Patankar, S. V., (1985), "Analysis of laminar mixed convection in shrouded arrays of heated rectangular blocks," Int. J. Heat Mass Transfer, Vol. 28, No. 9, pp. 1699-1709.

Bravo, R. H., (1991), "Development of the three-dimensional finite analytic method for simulation of fluid flow and conjugate heat transfer," Ph.D. Thesis, The University of Iowa, Iowa City, Iowa.

Chapman, A. J. (1987), "Fundamentals of heat transfer," Macmillan Publishing Co. New York.

Chen, C. J., Bravo, R. H. and Xu, Z., (1991), "Analysis of finite analytic discretization of incompressible three-dimensional Navier-Stokes equations," ASME Winter Annual Meeting, Atlanta, Georgia, December 1-6.

Fiveland, W. A., (1987), "Discrete ordinates methods for radiactive heat transfer in isotropically and anisotropically scattering media," J. Heat Transfer, Vol. 109, pp. 809-812.

Incropera, F. P., (1988), "Convection heat transfer in electronic equipment cooling," J. of Heat Transfer, November 1988, Vol. 110, pp. 1097-1111.

Patankar, S. V., Liu, C. H. and Sparrow, E. M., (1977), "Fully developed flow and heat transfer in ducts having streamwise-periodic variations of cross-sectional area," J. Heat Transfer, Vol. 99, pp.180-186.

Sanchez, A. (1991), "General purpose radiative transfer model for application to remote sensing in multi-dimensional systems," Ph. D. Thesis, The University of Iowa, Iowa City, Iowa.

Sanchez, A. , Krajeswski, W. and Smith, T. F., (1990), "Statistical framework for validation of satellite-based global precipitation simulation; Part I: An atmospheric radiation model - The plane layer case," Progress report prepared for Grant NA89AA-D-AC195 for National Oceanic and Atmos. Admin.

Sanchez, A., Smith, T. F. and Krajewski, W. F., (1991), "ANDISOR3 program listing. Three-dimensional radiative model," Technical Report, METFS 90-011, The University of Iowa, Iowa City, Iowa.

Shaw, H. J., Chen, W. L. and Chen, C. K., (1991), "Study of the laminar mixed convective heat transfer in three-dimensional channel with a thermal source," J. of Electronic Packaging, Vol. 113, pp. 40-49.

Siegel, R. and Howell, J. R., (1981), "Thermal radiation heat transfer," Hemisphere Publishing Corporation, New York.

Smith, T. F., (1990), "Radiation heat transfer notes," Department of Mechanical Engineering, The University of Iowa, Iowa City, Iowa.

Sparrow, E. M., Baliga, B. R. and Patankar, S. V., (1977), "Heat transfer and fluid flow analysis of interrupted wall channels, with application to heat exchangers," J. of Heat Transfer, February 1977, pp. 4-11.

Sparrow, E. M., Niethammer, J. E. and Chaboki, A., (1982), "Heat transfer and pressure drop characteristics of arrays of rectangular modules encountered in electronic equipment," Int. J. Heat Mass Transfer., Vol. 25, No. 7, pp. 961-973.